What it takes to compute highly accurate rovibrational line lists for use in astrochemistry

Xinchuan Huang[1,2*], David W. Schwenke[3], Timothy J. Lee[4*]

[1]*SETI Institute, 189 Bernardo Avenue, Suite 200, Mountain View, CA 94043, USA*

[2]*MS 245-6, Astrophysics Branch, Space Science and Astrobiology Division, NASA Ames Research Center, Moffett Field, CA 94035, USA*

[3]*MS 258-2, NAS Facility, NASA Ames Research Center, Moffett Field, CA 94035, USA*

[4]*MS245-3, Planetary Systems Branch, Space Science and Astrobiology Division, NASA Ames Research Center, Moffett Field, CA 94035, USA*

*Corresponding Author: E-mail: Timothy.J.Lee@nasa.gov, Xinchuan.Huang-1@nasa.gov

Conspectus

We review the Best Theory + Reliable High-resolution Experiment (BTRHE) strategy for obtaining highly accurate molecular rovibrational line lists with InfraRed (IR) intensities. The need for highly accurate molecular rovibrational line lists is two-fold: a) assignment of the many rovibrational lines for common stable molecules especially those that exhibit a large amplitude motion, such as NH_3, or have a high density of states such as SO_2; and b) characterization of the atmospheres of exoplanets which will be one of the main areas of research in astronomy in the coming decades. The first motivation arises due to the need to eliminate lines due to common molecules in an astronomical observation in order to identify lines from new molecules, while the second motivation arises due to the need to obtain accurate molecular opacities in order to characterize the atmosphere of an exoplanet. The BTRHE strategy first consists of using high-quality *ab initio* quantum chemical methods to obtain a global potential energy surface (PES) and dipole moment surface (DMS) that contains the proper physics. The global PES is then refined using a subset of the reliable high-resolution experimental data. The refined PES then gives energy level predictions to an accuracy similar to the reproduction accuracy of the experimental data used in the refinement step in the interpolation region (i.e., within the range of the experimental data used in the refinement step). The accuracy of the energy levels will slowly degrade as they are extrapolated to spectral regions beyond the high-resolution experimental data used in the refinement step. However, because the degradation is slow, the predicted energy levels can be

used to assign new high-resolution experiments, and the data from these can then be used in a subsequent refinement step. In this way, the global PES eventually can yield highly accurate energy levels for all desired spectral regions including to very high energies and high J values. We show that IR intensities computed with the BTRHE rovibrational wavefunctions and the DMS can be very accurate provided one has minimized the fitting error of the DMS and tested the completeness of the DMS. Some examples of our work on NH_3, CO_2, and SO_2 are given to highlight the usefulness of the BTRHE strategy and to provide ideas on how to further improve its predictive power in the future. In particular, it is shown how successive refinement steps, once new high-resolution data is available, can lead to PESs that yield highly accurate transition energies to larger spectral regions. The importance of including non-adiabatic corrections to reduce the J-dependence of errors for H-containing molecules is shown with work on NH_3. Another very important aspect of the BTRHE approach is the consistency across isotopologues, which allows for highly accurate line lists for any isotopologue once one is obtained for the main isotopologue (which has more high-resolution data available for refinement).

Key References

- Huang, X.; Schwenke, D. W.; Lee, T. J. Rovibrational Spectra of Ammonia. Part I: Unprecedented Accuracy of a Potential Energy Surface used with Nonadiabatic Corrections. *J. Chem. Phys.* **2011**, 134, 044320.[1] *This paper reports the first global potential energy surface (PES) for a polyatomic molecule that yields J=0-6 energy levels with an uncertainty of 0.015 cm^{-1} for all experimentally determined bands at that time.*
- Huang, X.; Schwenke, D. W.; Tashkun, S. A.; Lee, T. J. An Isotopic-Independent Highly-Accurate Potential Energy Surface for CO_2 Isotopologues and an Initial $^{12}C^{16}O_2$ IR Line lists. *J. Chem. Phys.* **2012**, 136, 124311.[2] *This paper reports an isotopic-independent global PES for CO_2 that has a σ_{rms} = 0.016 cm^{-1} for 6873 J=0-117 experimental energy levels.*
- Huang, X.; Schwenke, D. W.; Lee, T. J. Highly Accurate Potential Energy Surface, Dipole Moment Surface, Rovibrational Energy Levels, and Infrared Line List for $^{32}S^{16}O_2$ up to 8000 cm^{-1}. *J. Chem. Phys.* **2014**, 140, 114311.[3] *This paper reports an isotopic-independent global potential energy surface for SO_2 that gives J=0-80 energy levels with an uncertainty of 0.013 cm^{-1} for all experimental bands contained in HITRAN.*
- Huang, X.; Schwenke, D. W.; Lee, T. J. Exploring the Limits of the Data-Model-Theory Synergy: 'Hot' MW Transitions for Rovibrational IR Studies. *J. Mol. Struct.* **2020**, 1217, 128260.[4] *This paper explores ways to improve even further the prediction accuracy of the Best-Theory + Reliable High-resolution Experiment (BTRHE) strategy based PES refinements using experimental data from high-resolution rotational and rovibrational spectroscopic studies.*

I. INTRODUCTION

There are two areas in astronomical research that are fueling the need for ever more accurate and complete rovibrational molecular line lists. The first involves the increasing precision and spectroscopic accuracy of ground, airborne, and space-based telescopes. Ground-based telescopes include the Atacama Large Millimeter Array (ALMA), the NASA Infrared Telescope Facility (IRTF) with the TEXES instrument, and the Very Large Telescope (VLT) with the CRIRES+ instrument, while the EXES instrument on the Stratospheric Observatory for Infrared Astronomy (SOFIA) airborne platform is similar to the TEXES instrument. Recent space-based

telescopes include the HiFi instrument on the Herschel Space Observatory (HSO) as well as instruments on the Venus Express mission. The motivation behind these studies is to be able to identify all the rovibrational lines that belong to a stable, common molecule, such as H_2O or CO_2, or other stable common molecules that exhibit a large amplitude motion, such as NH_3, or have a high-density of states, such as SO_2. Once all the lines of these molecules are assigned, the remaining lines can be analyzed to determine if there are new previously unidentified molecules in the astrophysical environment being examined. The astrochemistry community has termed this approach as assignment of the rovibrational lines of weeds so that one may try to identify flowers in the remaining lines.[1-3]

The second area of research involves the characterization of the atmospheres of exoplanets as well as some of the planets and moons in our solar system. This area is exploding since the Kepler, K2, and TESS missions have dramatically expanded the number of known exoplanets, especially smaller rocky exoplanets. It is widely accepted that the next phase in the study of exoplanets will be to characterize their atmospheres, through their opacities, to try and understand the nature of the exoplanet,[5,6] with one of the ultimate goals to infer whether alien life might exist there. There are several factors that go into determining accurate opacities, including the rovibrational line lists discussed in this review, but also line shape parameters, temperature dependent broadening coefficients, and others as discussed in Refs. 5 and 6. In the near term, the James Webb Space Telescope (JWST) will provide the best opportunity to characterize the atmospheres of exoplanets, but it is clear that there is a significant need for accurate and complete rovibrational line lists for many more molecules.[5-7] Moreover, most of the exoplanets that JWST can characterize will by necessity be close to their parent star (possibly tidally locked), and will therefore be very hot, in the range of 1500 K to 3000 K. This means that the line lists need to extend to very high energies since the molecules will be highly rovibrationally excited, and depending on the nature of the exoplanet, the molecules of interest will mainly be stable such as H_2O, CO_2, SO_2, NH_3, and CH_4.[5-7] For M-dwarf stars, which are much cooler than Sun-like stars, there is the possibility of finding small rocky exoplanets that may be in the habitable zone, thus work has begun to identify and obtain low-temperature rovibrational line lists for possible biosignature or technosignature molecules.[8-12] In this case, the line lists need to be accurate and complete up to about 350 K.

There are significant differences between these two areas of research. In the first area of study, these molecules will mostly be identified in relatively cool environments, ranging from ~10 K to ~350 K, such as the interstellar medium (ISM), while much higher temperatures will be common in exoplanets studies, as indicated. In order to obtain reasonably accurate opacities in the hotter environment, hundreds of million or billions of rovibrational lines, with their intensities, are needed.[13,14] Though in some cases when identifying a specific molecule, the temperatures can also be high and a very good example of this was assigning spectroscopic rovibrational lines to the H_2O molecule in a sunspot at ~3500 K.[15] Needless to say, the spectrum of H_2O at 3500 K is very different to the one at 300 K.

Our first foray into computing accurate molecular rovibrational line lists started with NH_3 in 2008,[1,16-19] though it should be noted that the first effort at NASA Ames started in the 1990s with the H_2O molecule.[13,20] Thus far, we have had significant success in computing accurate and complete line lists for NH_3,[1,16-19] CO_2,[2,4,21-25] and SO_2,[3,25-30] and their isotopologues, though even for these molecules there is still work to be done extending the line lists to higher temperatures and improving the accuracy for higher energy levels. We have adopted a strategy that we call Best Theory + Reliable High-resolution Experiment (BTRHE) wherein we use very high levels of *ab initio* electronic structure theory to compute a potential energy surface (PES) and dipole moment surface (DMS), followed by empirical refinement of the PES using reliable high-resolution experimental data while solving the nuclear Schrödinger equation variationally. Typically, we use less than 500 experimental energy levels in the refinement stage, but it is critical that they be very accurate. With this approach, we have found that *all* other energy levels, that fall within the range of the experimental data used in the refinement step, will be as accurate as the reproduction of the experimental data used in the refinement. Energy levels extrapolated beyond the experimental data will slowly degrade. However, these data can be used to assign new high-resolution experiments, which then can be used in another refinement step of the PES to improve the performance at higher energies, which we have done.[19] In this way, one can eventually build a rovibrational line list that will be accurate and complete to very high temperatures. While this review is limited to our work on rovibrational line lists, we should mention that there are two other groups working in this arena as well, the ExoMol group,[14] and the Tyuterev group,[31] who use similar approaches but are implemented differently. Details of our approach are given in the following sections with highlights and conclusions that we have obtained through these studies.

II. ELECTRONIC STRUCTURE METHODS

Since the molecules that commonly occur in planetary atmospheres are stable, the obvious choice for a reliable and not too costly electronic structure method is the singles and doubles coupled cluster method including a perturbational estimate of connected triple excitations, denoted CCSD(T),[32-34] because thousands of points are needed for the PES and DMSs. Hence CCSD(T) is the base method used, but more corrections are incorporated through a composite scheme we developed for computing quartic force fields.[35-37] A large fraction of the remaining error in a CCSD(T) calculation will be that the basis set is not complete, so we extrapolate to the basis set limit using a three-point formula, denoted (TQ5).[38] Next, it is important to include the effects of core-correlation, which are computed with the Martin-Taylor (MT) basis sets.[39] The effects of scalar relativity are also included as a correction using the Douglas-Kroll (DK) formulation with the specialized DK basis sets, denoted TZ-DK.[40,41] When necessary, a higher-order valence correlation correction can be included using the averaged coupled-pair functional (ACPF) method.[42] Dunning's correlation-consistent basis sets are used denoted TZ, QZ, and 5Z, sometimes with diffuse functions or recontractions.[43,44] Eq. (1) shows a general formula for how the total electronic energy is computed for each grid point:

$$E_{Tot} = E_{TQ5} + \left(E_{MT,core} - E_{MT}\right) + \left(E_{TZ-DK,rel} - E_{TZ-DK}\right) + \left(E_{ACPF} - E_{CCSD(T)}\right) \qquad (1)$$

As mentioned, each PES and DMS will contain hundreds or thousands of points, and these generally will not be the same points for each. When computing the DMS, we start with the same list of points, but it is necessary to have a tighter grid of points when the surface is changing more rapidly, and this is usually not in the same place for the PES and DMS, thus completeness tests of the DMS are required. Eq.(1) can be used for both the PES and DMS as the DMS is computed as the numerical gradient of the energy with respect to an external electric field.[1-3,16,21] All the electronic structure calculations performed in these studies used the MOLPRO quantum chemistry package.[45]

III. CONSTRUCTION OF THE POTENTIAL ENERGY SURFACE

a. FUNCTIONAL FORM OF THE PES

In our methods, we require an analytic representation of the results of the electronic structure calculations. We try to build as much physics as possible into the analytic representation by splitting the PES into zero-order term, V_{long}, and a correction term, V_{short}. Thus, $V = V_{long} + V_{short}$.

The zero-order term represents the asymptotic limits as well as the highly repulsive regions of the potential, and this can be most conveniently achieved by using atom-atom distances. The correction term is taken as a polynomial of physically motivated internal coordinates, such as stretches and bends, multiplied by a damping factor that ensures that the polynomials do not lead to unphysical minima in the final PES. For bending coordinates for triatomic molecules, we use the cosine of the bending angle in our polynomial expansions to ensure the proper physical behavior at the ends of the coordinate range.

When we carry out the rovibrational calculations,[49] in order to evaluate the matrix elements of the PES, we re-expand the angular dependence in terms of basis functions for which we can analytically evaluate the angular matrix elements. These basis functions will be the same as the angular basis used to expand the rovibrational wavefunction for total angular momentum zero. This re-expansion is done by quadrature by projecting our expansion basis on the PES. If the PES does not obey the physical boundary conditions, *i.e.* if we used the bending angle rather than the cosine of the bending angle, this quadrature would never converge and the results one obtained would depend sensitively on the quadrature parameters used.

b. **FITTING THE PES**

For closed shell molecules, second-order Møller-Plesset perturbation theory (MP2) energies with the aug-cc-pVTZ basis set are computed on a loose but full-dimensional geometry grid and fit to a 4^{th} – 8^{th} order polynomial. This allows us to constrain the number of points needed for high quality *ab initio* calculations in every 1500 – 5000 cm^{-1} range, which are randomly chosen from a set of 100K to 1 million geometries generated in the primitive fit.

The expensive high-level *ab initio* calculations require very high fitting accuracy in the spectroscopically important region. After identifying unreliable data and high energy regions to avoid or ignore, we test various basis functions and tweak weighting and damping functions to minimize σ_{rms}.[3,13,16] We reported σ_{rms} = 0.1-0.3 cm^{-1} for hundreds or thousands of CO_2, SO_2 and NH_3 points below 30,000 – 40,000 cm^{-1}.[2,3,16] These were achieved by sacrificing the fitting accuracy at higher energies.

The hardest step is adding boundary points to ensure the fit is globally positive, smooth, *and* still has a reasonable σ_{rms}. We can accomplish this by running additional *ab initio* calculations, extrapolating a 2^{nd}-4^{th} order approximation in Morse-trigonometry coordinate system,[46,47] then fit together with 1/500 ~ 1/100 of normal weights. An optimal choice of boundary point energies and weights can significantly reduce the effort for this step.

We compute J=0 band origins on the series of PESs determined from various *ab initio* energies, extrapolations, corrections, and their combinations. These are compared with experimental data *collection* to choose a good starting PES, with a few cm^{-1} deviations. Our NH_3 starting PES was basis set limit + diagonal Born-Oppenheimer correction + 50% ACPF/TZ correction,[16] while our SO_2 and CO_2 starting PESs were QZ based.[2,3]

It may take many months to get a good starting PES for the following variational computations. Procedures should be automated as much as possible, especially for the boundary point processes.

We do not recommend shifting the minimum geometry to match band origins, but it is possible. The true minimum of our starting PES should be close to the *real* or experimental minimum structure, but it cannot be used as a reference in the short-range potential expansion because the minimum geometry is part of the refinement algorithm.[13]

c. EMPIRICAL REFINEMENT OF THE PES

On the selected PES, the derivatives of the energies with respect to the PES coefficients are computed from tightly converged rovibrational wavefunctions. Every experimental level is matched to a specific eigenvalue, which we can track and quickly update without expensive rovibrational calculations. Usually these matrices should have energy cutoff at least 3000 – 5000 cm^{-1} above the highest energy level to be refined. If the Hamiltonians were not tightly converged, the reference energies need adjustments. Note that different isotopologue data can be refined together, if they are not heavily impacted by nonadiabatic effects.

To achieve σ_{rms}< 0.05 cm^{-1}, the importance of using only reliable high-resolution *experimental* data cannot be overstated. During CO_2 refinement, using HITRAN2008[48] data introduced errors > 0.1 cm^{-1}. Only actual experimental data led to σ_{rms}=0.01-0.02 cm^{-1} for 6873 experimental levels (J=0-117, and E<13,000 cm^{-1}).[2] Avoid incomplete effective Hamiltonian (EH)

models or extrapolation unless necessary. Data quality predetermines the refinement quality, σ_{rms}, and prediction accuracy.

As shown in Fig.1, the first two rounds of refinement reduce the band origin deviations and minimize the J (and/or K) dependence of energy level deviations. We start with J=0 band origins, then from lower J to higher J. Uniform prediction accuracy for isotopologues may include mass-dependent corrections and other higher-order effects, if necessary.

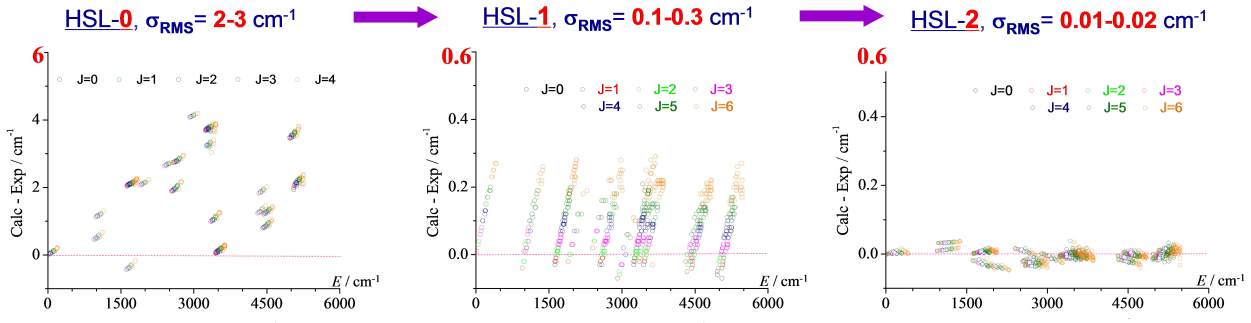

Fig.1. Two orders of magnitude error reduction by BTRHE refinement, for the accuracy of $^{14}NH_3$ rovibrational energy levels from the HSL-0 to HSL-1 to HSL-2 PESs. Reproduced with permission from Ref.1. Copyright 2011 AIP Publishing.

Fitting to energy levels *or* transitions may depend on the focus. We usually choose ~500 experimental energy levels, and more if needed for higher J/energy. Use of thousands of levels is hard to track. It is critical to assign proper weights to balance the accuracy across the J and energy range. The refined σ_{rms} on the selected refinement set should be very similar (within ±20%) to the σ_{rms} for the whole experimental dataset (> 6000 ~ 12,000 levels or transitions), i.e. ±0.01 – 0.03 cm^{-1}.[1-3,16]

At first, some levels matched with inaccurate quantum numbers are hard to refine so their weights should be minimized. In the end, when everything is done properly, energy levels that do not match usually suggest errors in their energies or assignments, but an energy level successfully used in the refinement is *not* necessarily real as discussed in Ref.23.

For H_2O to SO_2, we refine the 0^{th} – 4^{th} order V_{Short} terms because they have the most dominant contributions. Tests showed sextic order terms may further reduce σ_{rms} by ~30% but with tripled effort. Since the starting PES is already close to spectroscopic accuracy, all refinements should be a small change on the original V_{Short} coefficients, e.g. a few percent or less.[1-3,16] We recommend constraining the parameter ranges and redistributing the refinement effect over the whole PES coefficient set to avoid over-refinement.[1-3]

The prediction accuracy of the post-refinement PES relies on several factors. For example, molecular complexity and data coverage are different; extrapolation accuracy gradually shifts to that of the original *ab initio* surface; states in strong coupling or resonance are easier to predict than isolated ones.

Relative to localized EH models, our predictions provide much more complete, reliable, and consistent reference for experiments. New reliable high-resolution experiments help improve the refinements, and further enhance the predictions in unexplored regions. See our NH_3 study at 1.5 μm.[19] Such mutually beneficial interaction with experimentalists may last many cycles.

IV. ROVIBRATIONAL CALCULATIONS

a. VARIATIONAL CALCULATIONS WITH AN EXACT KINETIC ENERGY OPERATOR

All our calculations use coordinates for which the Born-Oppenheimer kinetic energy operator can be written in closed form. These coordinates are generated by starting with the nuclear cartesian position vectors, then multiplying by a mass transformation matrix from a set of cartesian internal vectors plus the cartesian center of mass vector.[49] The cartesian center of mass vector then can be dropped from the formulism. The internal cartesian vectors are then transformed into spherical polar coordinates in a laboratory fixed frame of reference. The angular coordinates are then transformed to body fixed angles plus three Euler angles. The Euler angles specify the overall orientation of the system. This mass transformation matrix can yield either orthogonal coordinates, in the sense that the kinetic energy operator in the cartesian internal vectors has no cross terms, or the transformation can be more general. For either case, the kinetic energy operator can be easily written down in closed form,[50] albeit in the non-orthogonal case there are many more terms to consider.

For triatomic molecules, there are only two unique orthogonal coordinate sets: Jacobi coordinates or Radau coordinates. In our calculations, we use Radau coordinates, for they lead to easy exploitation of the symmetry resulting from identical nuclei without leading to strong correlation between the coordinates. For an example of the latter, if one were to use $O+H_2$ Jacobi coordinates on calculations of the water molecule, one would have to treat the situation where the O atom approaches the center of mass of the H_2 very carefully, for in order to maximize the flexibility of the wavefunction, the radial-bending function must go as $r^{J+1} P_{lK}(\cos\chi)$, where r is

the O to center of mass H_2 distance, P_{lK} is an associated Legendre function, and χ is the angle between the two vectors.[51] Similar considerations occur for larger molecules.[1,16]

We represent the radial functions in terms of contracted analytic basis functions[52] rather than numerical functions.[49] Besides improving the efficiency of the calculations, it also avoids the problem that numerical functions have when computing high overtone intensities.[49]

Matrix elements of the PES are evaluated via optimized quadrature over the radial functions[49] while the angular integrations are carried out by re-expansion, as described above. A recent improvement in our methods is to switch to a much more accurate method for computing the optimized quadrature weights and nodes.[53] This has enabled us to significantly push the computation accuracy of the PES matrix elements and hence the final rovibrational energies and wavefunctions. It should be noted that this procedure is applicable only for a PES that has smooth high order derivatives. Thus, converged matrix elements are not possible, for example, for a PES represented in terms of spline functions, or for a PES with rapidly varying switching functions.

b. INCLUSION OF NON-ADIBATIC CORRECTIONS

It has been known since the work of Wolniewicz[54] on the H_2 molecule that one must go beyond the Born-Oppenheimer approximation (BOA) for high accuracy predictions. Empirical calculations[55] on the H_2 molecule showed that these non-adiabatic corrections would be well approximated by using the atomic reduced mass in the vibrational part of the kinetic energy operator and the nuclear reduced mass in the centrifugal part of the kinetic energy operator. This observation has led many researchers to use atomic masses in all parts of the kinetic energy operator in their rovibrational calculations, even though the proper masses to use within the BOA are the nuclear masses. The use of one mass in the vibrational part of the kinetic energy operator and another in the rotational part of the kinetic energy operator for polyatomic molecules is not possible because these motions are not decoupled the way they are for diatomic molecules. A big advance in this situation was the development of a practical *ab initio* method to compute these corrections for polyatomic molecules.[56] The resulting correction to the BOA is a kinetic energy like term that consists of first derivative and second derivative operators, with the latter including cross derivatives even though the Born-Oppenheimer kinetic operator does not contain cross derivatives, and the coefficients for these operators are geometry dependent. This, of course, is a signification complication compared to the BOA, but at least for the case of the H_2O molecule,

results of reasonable accuracy can be obtained by only including the derivative operators that are already present in the BOA and to use constant coefficients determined at the equilibrium geometry.[56] Some averaging may be required to ensure that identical nuclei symmetry is retained, and we have done so in our calculations for CH_4[57] and NH_3.[1]

A recent advance has enabled us to compute these terms using analytic differentiation of the electronic wavefunction.[58] This provides a huge speed up in the calculations of these terms, both because analytic derivatives require significantly less work than accurate numerical ones and because one can use the full symmetry even for non-totally symmetric derivative terms.

Most of our recent work has been with linear triatomic molecules. In these situations, our analytic representation[56] of the non-adiabatic corrections is not used because they diverge at linear geometries. Subsequent careful work[59] on the form of the kinetic energy operator for open-shell systems contains the ideas required to resolve that dilemma.

V. COMPUTING INFRARED INTENSITIES

a. CONSTRUCTION OF THE DIPOLE MOMENT SURFACE

Many DMSs have dipole components fitted separately, e.g. a NH_3 DMS.[60] We believe the permutation invariance is critical for polyatomic DMSs, so we fit the pseudo point charges on nuclei. Our NH_3, CO_2 and SO_2 DMSs use a single polynomial expansion for q_H or q_O, with the N, C or S atom at the origin.[2,3,16] For CO_2, we have

$$\vec{\mu} = q_{O1} \cdot \overrightarrow{r_{O1}} + q_{O2} \cdot \overrightarrow{r_{O2}} + q_C \cdot \overrightarrow{r_C} = q_{O1} \cdot \overrightarrow{r_{O1}} + q_{O2} \cdot \overrightarrow{r_{O2}},$$

$$q_{O1} = \sum_{n=1}^{969} C_{ijk}^{n} \Delta {r_1}^{i} \Delta {r_2}^{j} (1 + cos\angle_{OCO})^{k},\ q_{O2} = \sum_{n=1}^{969} C_{ijk}^{n} \Delta {r_2}^{i} \Delta {r_1}^{j} (1 + cos\angle_{OCO})^{k}.$$

This definition ensures the computed dipole properly transforms as a rank one tensor, something that fitting the components separately cannot achieve.[49] For molecules like N_2O or OCS, we need two polynomial expansions for the different ending atoms, with N or C at the origin.

Ab initio dipoles are computed as a numerical gradient of CCSD(T) electronic energies with external electric field strength set to 0.0001 a.u. or less. Target accuracy dictates the *ab initio* basis requirements. We recommend a QZ basis as a minimum for agreement greater than 90% for intensities. Appropriate basis sets may noticeably improve agreement with experiment, see Fig.2 of Ref.30. Dipole data requires a consistency check before the fits.[1-3,16,21] The weighting function

either focuses on lower energy, spectroscopically important regions, or applies uniform weights for limited range. The best dipole fitting basis could be different from that used in the PES.

We expect fitting accuracy to be better than 99.9%, i.e. average relative deviation < 0.1%. Fitting σ_{rms} reported for SO_2 and CO_2 were 3E-5 a.u. and 8E-6 a.u., respectively, for the 0 – 30,000 cm^{-1} range.[2,3] For higher-order overtones, a high fitting accuracy is important.

b. TESTING THE COMPLETENESS OF THE DMS

After securing a PES refinement with $\sigma_{rms} \leq 0.1\text{-}0.5$ cm^{-1}, we run intensity calculations with the DMS series constructed using different dipoles, energy cutoffs, fitting bases, fitting orders, and weighting functions, etc. The DMS quality can be estimated by intensity comparison against observations. But we need to go beyond that.

Fig.2 compares 4 different CO_2 DMSs.[21] The DMSs-N2/N3 show very similar agreements with all intensity data in HITRAN2008, but their predictions in 12000 – 15000 cm^{-1} diverge by 1-2 orders of magnitude. We chose DMS-N2 because its lower intensities and sharper band shapes may suggest smaller noise at high energies. Lower accuracy dipole fits usually contain more noise leading to fake intensities. Note all 4 DMSs agreed that the HITRAN2008 intensities in 8300-9200 cm^{-1} were off by two orders of magnitude. In short, our DMS tests help identify unreliable experimental data and a more reliable DMS for the whole range.

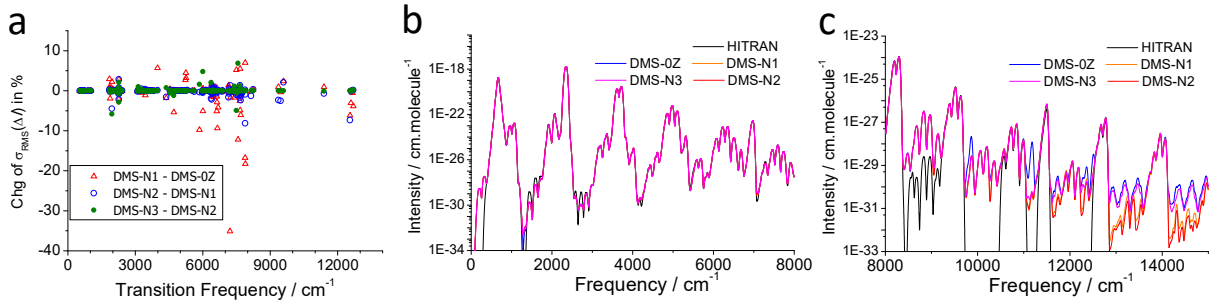

Fig.2. Compare CO_2 DMS-0Z and -N1/2/3 based 296K IR line lists, and HITRAN2008: (a) band intensity improvements and differences; (b) and (c), smoothed spectra (FWHM=8.3 cm^{-1}) in 0 – 8000 cm^{-1} and 8000–15,000 cm^{-1}. Reproduced with permission from Ref.21. Copyright 2013 Elsevier Inc.

The majority of experimental intensity data have uncertainties of 1-5%, sometimes even larger. Our line lists have far better isotopologue consistency than EH/EDM based line lists.[23] Recent systematic investigations show our consistency level to be 99.9% or higher.[25] Fig.3 gives two examples for SO_2 and CO_2. We believe that in the future, if the experimental uncertainty of

IR intensities is small enough, we can further "calibrate" or "refine" our intensity predictions. We can also use reliable experimental intensities to identify DMS deficiencies and try fixing them by adding additional points into the DMS fit. However, we do not really know how to "refine" a dipole surface analytically.

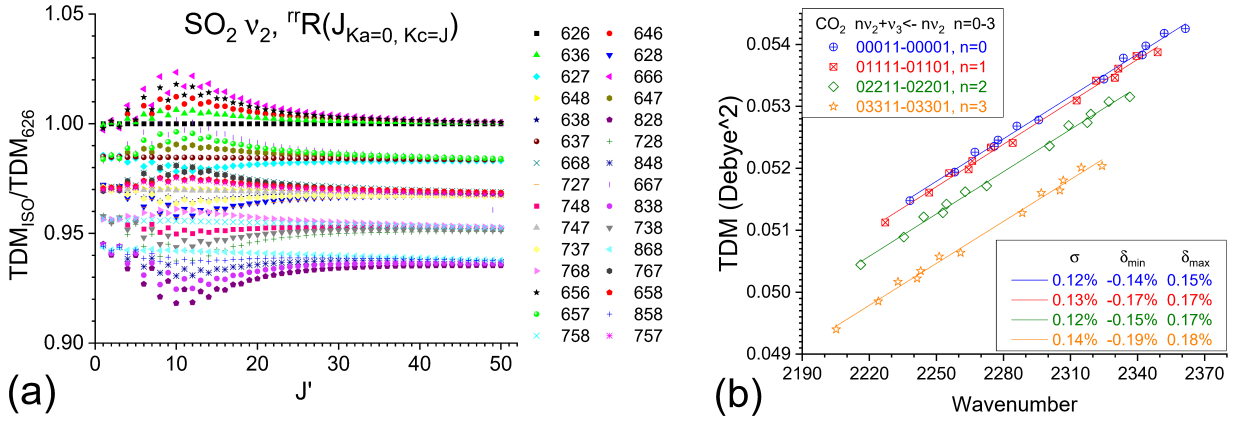

Fig.3. Isotopologue consistency of Ames IR list intensity: (a) SO_2 Isotope effects on the Transition Dipole Moments (TDM), ISO/626, for ν_2 ${}^{rr}R_{J=Kc,\,Ka=0}$ transition of 30 isotopologues. (b) The TDM of $n\nu_2+\nu_3 \leftarrow n\nu_2$ R16 transitions can be linearly approximated with <0.2% deviations for 13 CO_2 isotopologues. Reproduced with permission from Ref.25. Copyright 2019 Elsevier Inc.

VI. SELECTED HIGHLIGHTS IN APPLICATIONS TO NH_3, CO_2, AND SO_2

The $^{12}C^{16}O_2$ example in Fig.4 confirms σ_{RMS}= 0.01-0.02 cm^{-1} is realistic for refinements using pure experimental data.[2] Fig.5 shows similar accuracy for the experimental J=0 band origins of minor isotopologues, while 1-10 cm^{-1} uncertainties exist in high energy region.[23]

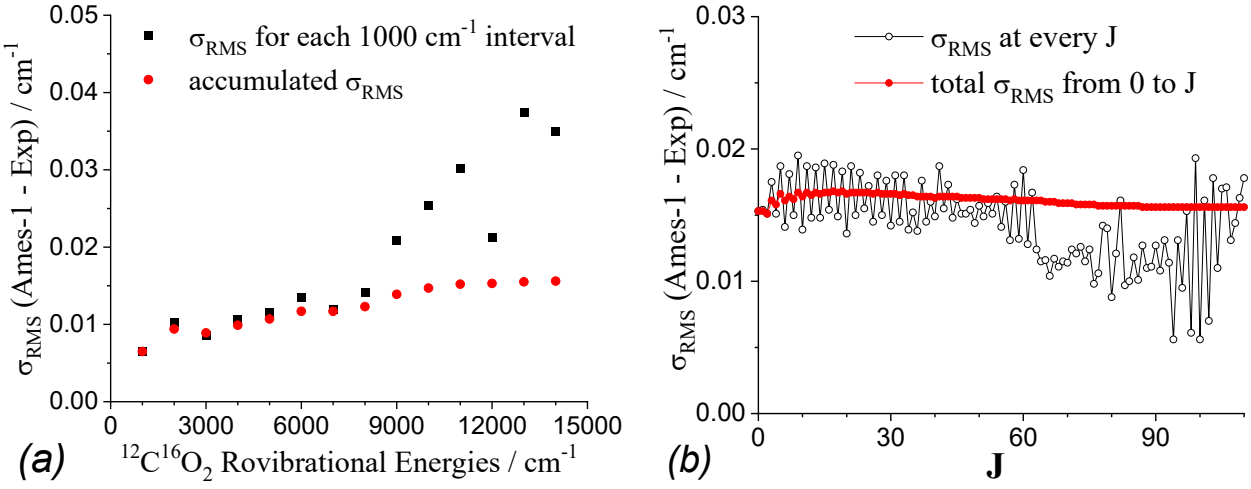

Fig.4. Fitting deviations on $^{12}C^{16}O_2$ Ames-1 PES refinement in a) each 1500 cm^{-1}; b) every *J in 0*-117. Reproduced with permission from Ref.2. Copyright 2012 AIP Publishing.

When EH model extrapolations break down beyond their experimental data range, our predictions can still be reliable. Fig.6a demonstrates how an SO_2 EH model deteriorates exponentially at high K_a.[3] Fig.6b plots the $\delta_{Calc-Expt}$ of $^{12}C^{16}O_2$ 60025 band[61] at ~12,500 cm^{-1}, Ames[23] vs CDSD2019.[62]

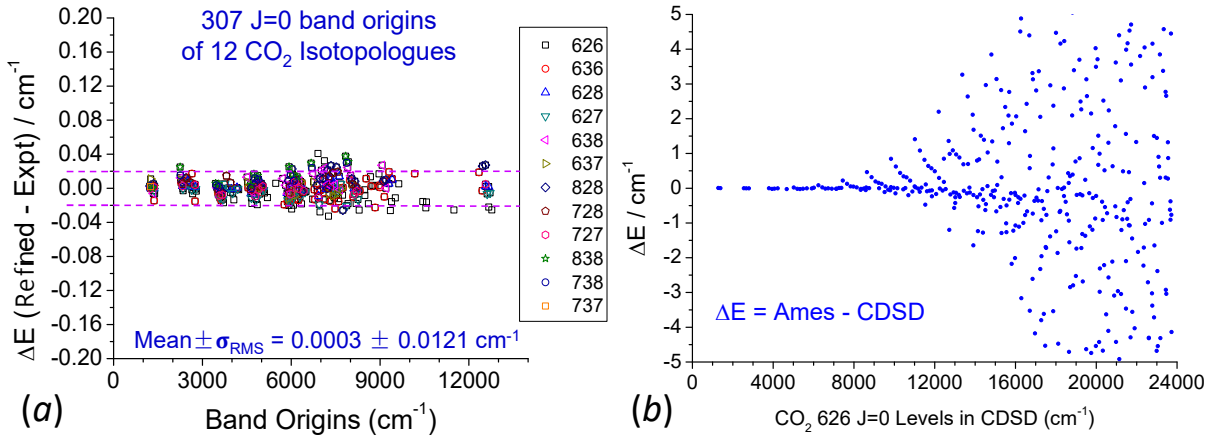

Fig.5. a) Measured vibrational band origin reproduction accuracy for 12 CO_2 isotopologues on Ames-2 PES; b) J=0 energy differences between Ames-2 predictions and CDSD EH model extrapolations. Reproduced with permission from Ref.23. Copyright 2017 Elsevier Inc.

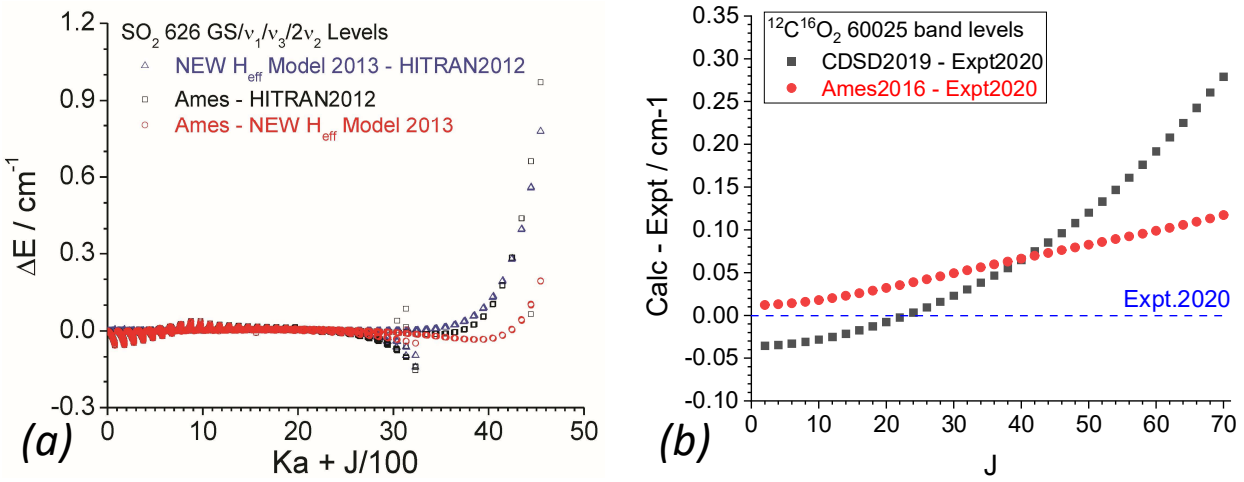

Fig.6. a) Compares $^{32}S^{16}O_2$ predictions, Ames vs. old EH model (HITRAN2012, K_a≤23), and 2013 EH Model (K_a≤35). Reproduced with permission from Ref.3. Copyright 2014 AIP Publishing. b) Prediction error δ(Calc – Expt) for $^{12}C^{16}O_2$ 60025 band at ~12,500 cm^{-1}, with Expt. data from ref.61.

Comparing to experiments, our prediction reliability has been confirmed for some weak bands, high temperature simulations, and mixed isotopologue analyses, see Fig.7. Note we did not

target <1% intensity deviations, but still have agreement with highly accurate CO_2 intensity measurements.

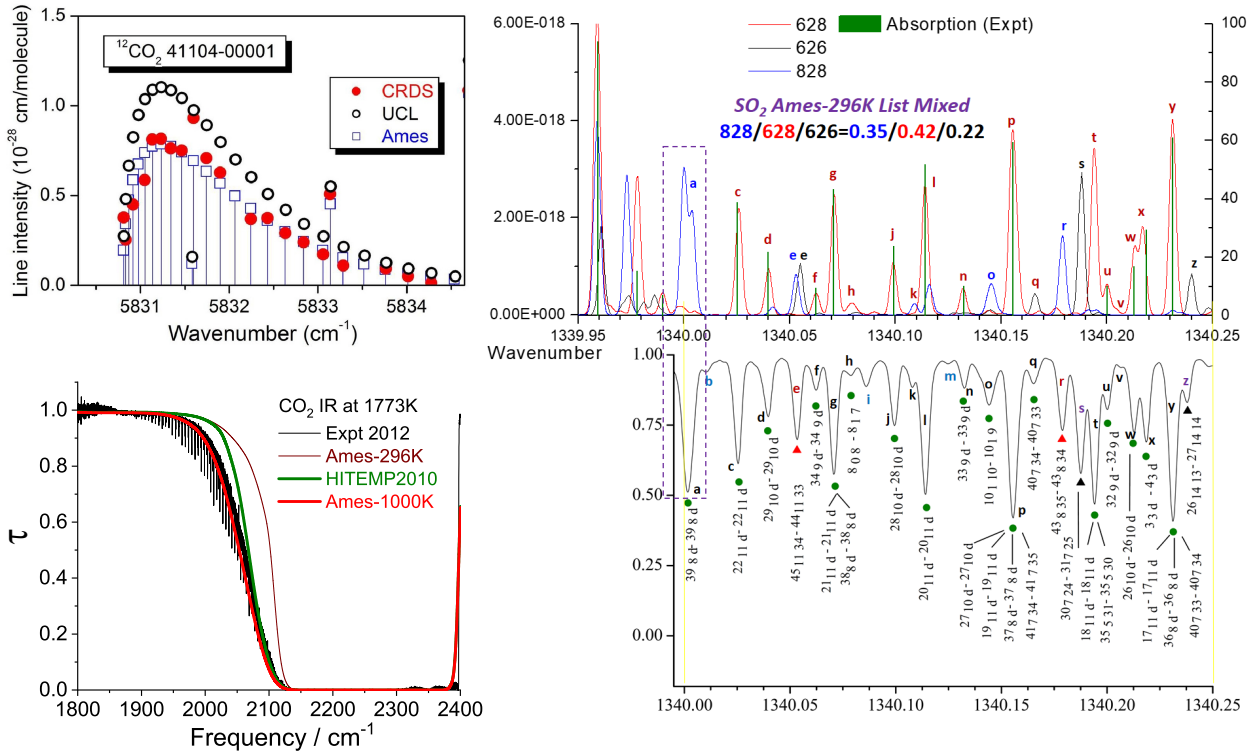

Fig.7. (Left top): Stick spectra overview of $^{12}C^{16}O_2$ 41104-00001 band, Expt/CRDS (red) vs Ames (squares). Reproduced with permission from Ref.63. Copyright 2018 Elsevier Inc. (Left bottom): Ames-1000K $^{12}C^{16}O_2$ line list (red) simulation vs. Experiment (black) at 1773K (Ref.64) Adapted with permission from Ref.21. Copyright 2013 Elsevier Inc. (Right): High-resolution IR analysis involving 3 SO_2 isotopologues, Ames-296K Simulation (top) vs Experiment (bottom), in 0.25 cm^{-1}. See details in Ref.28. Adapted with permission from Refs.28 and 65. Copyright 2016 Elsevier Inc.

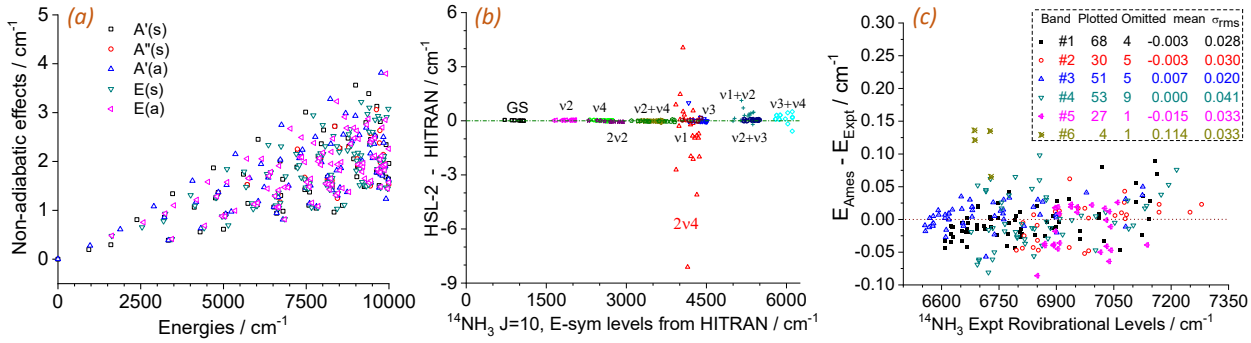

Fig.8. (a) Nonadiabatic effects on NH_3 J=0 levels, estimated on HSL-2 PES. Reproduced with permission from ref.1. Copyright 2011 AIP Publishing; (b) Ames HSL-2 PES vs. old HITRAN model differences for NH_3 bands at J=10. Reproduced with permission from Ref.18. Copyright 2011 AIP Publishing; (*c*) Agreement between Ames HSL-Pre3 PES and six NH_3 bands observed at 1.5 μm. Adapted with permission from Ref.19. Copyright 2012 Elsevier Inc.

With non-adiabatic corrections included (Fig.8a), our NH_3 study[1,18] found old EH models for the $2\nu_4$ state needs improvement (Fig.8b). In Fig.8c, we were able to extend the 0.02-0.04 cm^{-1} accuracy to 7000 cm^{-1} when new experimental data became available.[19]

Predictions may be further improved by using *the most accurate* experimental EH parameters to refine the *A/B/C* and quartic terms fitted from BTRHE line lists.[4,25] In the SO_2 vibrational ground state, isotopic effects of rotational constants (Fig.9a) and quartic centrifugal distortion constants (Fig.9b) follow simple mass relations. The isotopologue MW accuracy in benchmark test[25] reached ±1-5MHz at low J/K_a (Fig.9c).

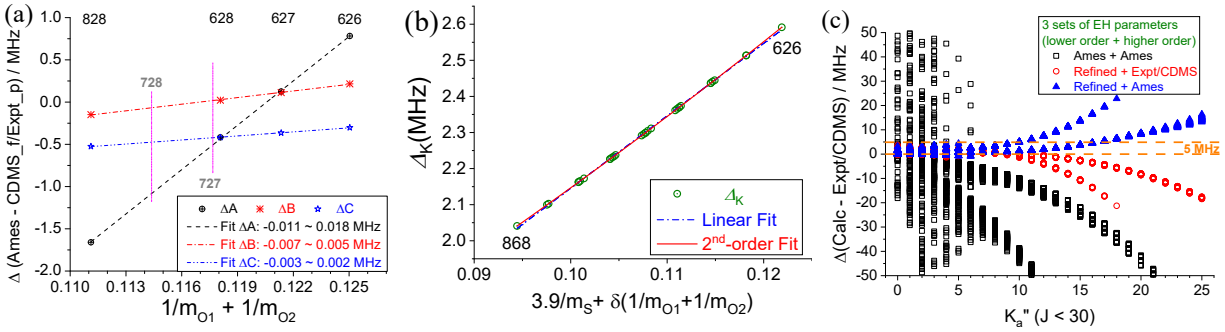

Fig.9. Benchmark study on SO_2 MW Spectra: (a) $^{17/18}O$ effects on *A/B/C* constants can be predicted within 0.01-0.02 MHz; (b) Δ_K approximation for 30 isotopologues, σ_{RMS} = 2.5 kHz (linear) or 0.37 kHz (2^{nd}-order); (c) Ames $^{34}S^{16}O_2$ MW list accuracy is improved when EH_{Ames} lower-order terms are "Refined" using $\delta_{Ames-Expt}$ deviations of $^{32/33}S^{16}O_2$. Adapted with permission from Ref.25. Copyright 2019 Elsevier Inc.

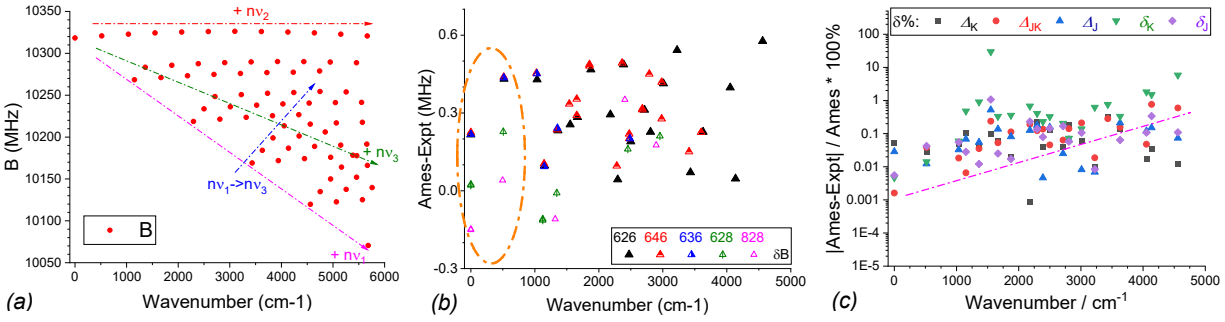

Fig.10. (a) Vibrational dependence of the *B* constants of $^{32}S^{16}O_2$; (b) $\delta_{EH(Ames)\,-\,EH(Expt)}$ difference of *B* constants of 5 SO_2 isotopologues; (c) relative difference δ% = 100%×δ/EH(Ames) of 5 quartic EH($^{32}S^{16}O_2$). Adapted with permission from Ref.4. Copyright 2020 Elsevier Inc.

Vibrational excitation effects on SO_2 *lower order* EH parameters are also investigated. Fig.10a shows *B* variations. In principle, we can still refine them, but the inconsistency among EH(Expt) models make the $\delta_{Ames\text{-}Expt}$ differences unsuitable for modeling and predictions.[4] Need more consistent EH(Expt) parameters, as Figs.10b and 10c suggest.

VII. Concluding Remarks

In this review, we have demonstrated that the BTRHE approach yields highly accurate and complete rovibrational line lists for molecules. When done properly, the prediction accuracy of the energy levels will be similar to the refinement accuracy, and it will degrade slowly as one extrapolates into spectral regions not covered by the experimental data. IR intensities also can be determined very accurately, generally to $\delta \leq 5\%$, and in many cases to 1-2% or better. The excellent predictive nature and consistency of the Ames IR line lists and rovibrational energy levels should contribute to new spectra analysis, EH model improvements, and IR simulations involving high temperatures, high energies, and isotopologues. New experimental data $\leftrightarrow$ New PES refinement (line list) is the ideal path.

Biographical Sketches

Xinchuan Huang is a SETI research scientist working in the Astrophysics Branch at NASA Ames Research Center. He received a B.S. in Applied Chemistry (II) from Fudan University in 1997 and a Ph.D. in Physical/Theoretical Chemistry from Emory University in 2004. He joined the Carl Sagan Center of Research at the SETI Institute after one-year postdoc at Emory (2004-2005) and three-year NASA Postdoctoral Fellowship (2006-2009) at Ames. His research interests are computational spectroscopy and IR line lists for astronomically and atmospherically important molecules.

David W. Schwenke is a senior research scientist in the NAS Facility at NASA Ames Research Center. He obtained his Ph.D. in Chemistry from the University of Minnesota. He arrived at NASA Ames in 1987 and became a civil servant in 1988. His research interests include development of methods in variationally solving the nuclear Schrödinger equation and in

electronic structure theory, and in applying these to chemistry and physics problems in the areas of aeronautics research and space science research.

Timothy J. Lee is a senior research scientist in the Space Science & Astrobiology Division at NASA Ames Research Center where he was previously Division Chief for 10 years. He received a Ph.D. in Chemistry from the University of California, Berkeley. He postdoc'ed at Cambridge University, and arrived at NASA Ames in 1988 becoming a civil servant in 1989. He is past Chair of the Astrochemistry Subdivision of the Physical Chemistry Division of the ACS. His research interests include development of quantum chemistry methods, with applications in astrochemistry, atmospheric chemistry, and molecular spectroscopy including rotational, vibrational, rovibrational, and electronic.

Acknowledgements

The authors gratefully acknowledge support from the NASA 17-APRA17-0051, 18-APRA18-0013, and 18-2XRP18_2-0046 grants. NASA/SETI Institute Cooperative Agreements NNX17AL03G, 80NSSC19M0121 have funded the work undertaken by X.H.

References:

1. Huang, X.; Schwenke, D. W.; Lee, T. J. Rovibrational Spectra of Ammonia. Part I: Unprecedented Accuracy of a Potential Energy Surface used with Nonadiabatic Corrections. *J. Chem. Phys.* **2011**, 134, 044320.
2. Huang, X.; Schwenke, D. W.; Tashkun, S. A.; Lee, T. J. An Isotopic-Independent Highly-Accurate Potential Energy Surface for CO_2 Isotopologues and an Initial $^{12}C^{16}O_2$ IR Line lists. *J. Chem. Phys.* **2012**, 136, 124311.

3. Huang, X.; Schwenke, D. W.; Lee, T. J. Highly Accurate Potential Energy Surface, Dipole Moment Surface, Rovibrational Energy Levels, and Infrared Line List for $^{32}S^{16}O_2$ up to 8000 cm^{-1}. *J. Chem. Phys.* **2014**, 140, 114311.
4. Huang, X.; Schwenke, D. W.; Lee, T. J. Exploring the Limits of the Data-Model-Theory Synergy: 'Hot' MW Transitions for Rovibrational IR Studies. *J. Mol. Struct.* **2020**, 1217, 128260.
5. Fortney, J. J.; Robinson, T. D.; Domagal-Goldman, S.; Amundsen, D. S.; Brogi, M.; Claire, M.; Crisp, D.; Hebrard, E.; Imanaka, H.; de Kok, R.; Marley, M. S.; Teal, D.; Barman, T.; Bernath, P.; Burrows, A.; Charbonneau, D.; Freedman, R. S.; gelino, D.; Helling, C.; Heng, K.; Jensen, A. G.; Kane, S.; Kempton, E. M.-R.; Kopparapu, R. K.; Lewis, N. K.; Lopez-Morales, M.; Lyons, J.; Lyra, W.; Meadows, V.; Moses, J.; Pierrehumbert, R.; Venot, O.; Wang, S. X.; Wright, J. T. The Need for Laboratory Work to Aid in The Understanding of Exoplanetary Atmospheres. **2016**, 1-18, http://arxiv.org/abs/1602.06305.
6. Fortney, J. J.; Robinson, T. D.; Domagal-Goldman, S.; Del Genio, A. D.; Gordon, I. E.; Gharib-Nezhad, E.; Lewis, N.; Sousa-Silva, C.; Airapetian, V.; Drouin, B.; Hargreaves, R. J.; Huang, X.; Karman, T.; Ramirez, R. M.; Rieker, G. B.; Tennyson, J.; Wordsworth, R.; Yurchenko, S. N.; Johnson, A. V.; Lee, T. J.; Dong, C.; Kane, S.; Lopez-Morales, M.; Fauchez, T.; Marley, M. S.; Sung, K.; Haghighipour, N.; Robinson, T.; Horst, S.; Gao, P.; Kao, D.; Dressing, C.; Lupu, R.; Savin, D. W.; Fleury, B.; Venot, O.; Ascenzi, D.; Milam, S.; Linnartz, H.; Gudipati, M.; Gronoff, G.; Salama, F.; Gavilan, L.; Bouman, J.; Turbet, M.; Benilan, Y.; Henderson, B.; Batalha, N.; Jensen-Clem, R.; Lyons, T.; Freedman, R.; Schwieterman, E.; Goyal, J.; Mancini, L.; Irwin, P.; Desert, J.-M.; Molaverdikhani, K.; Gizis, J.; Taylor, J.; Lothringer, J. Pierrehumbert, R.; Zellem, R.; Batalha, N.; Rugheimer, S.; Lustig-Yaeger, J.; Hu, R.; Kempton, E.; Arney, G.; Line, M.; Alam, M.; Moses, J.; Iro, N.; Kreidberg, L.; Blecic, J.; Louden, T.; Molliere, P.; Stevenson, K.; Swain, M.; Bott, K.; Madhusudhan, N.; Krissansen-Totton, J.; Deming, D.; Kitiashvili, I.; Shkolnik, E.; Rustamkulov, Z.; Rogers, L.; Close, L. The Need for Laboratory Measurements and Ab Initio Studies to Aid Understanding of Exoplanetary Atmospheres. 2019, 1-10, http://arxiv.org/abs/1905.07064.

7. Tennyson, J.; Yurchenko, S. N. Laboratory Spectra of Hot Molecules: Data Needs for Hot Super-Earth Exoplanets. *Mol. Astrophys.* **2017**, 8, 1-18.
8. Shields, A.L., Ballard, S., Johnson, J.A. The habitability of planets orbiting M-dwarf stars. *Physics Reports* **2016**, 663, 1–38.
9. Schwieterman, E.W.; Kiang, N.; Parenteau, M.N.; Harman, C.E.; DasSarma, S.; Fisher, T.M.; Arney, G.N.; Hartnett, H.E.; Reinhard, C.T.; Olson, S.L.; Meadows, V.S.; Cockell, C.S.; Walker, S.I.; Grenfell, J.L.; Hegde, S.; Rugheimer, S.; Hu, R.; and Lyons, T.W. Exoplanet biosignatures: A review of remotely detectable signs of life. *Astrobiology* **2018**, 18, 663-708.
10. Meadows V. S.; Reinhard C. T.; Arney G. N.; Parenteau M. N.; Schwieterman E. W.; Domagal-Goldman S. D.; Lincowski A. P.; Stapelfeldt K. R.; Rauer H.; DasSarma S.; Hegde S.; Narita N.; Deitrick R.; Lustig-Yaeger J.; Lyons T. W.; Siegler N.; Grenfell J. L. Exoplanet Biosignatures: Understanding Oxygen as a Biosignature in the Context of its Environment. *Astrobiology* **2018**, 18, 630-662.
11. Catling D. C.; Krissansen-Totton J.; Kiang N. Y.; Crisp D.; Robinson T. D.; DasSarma S.; Rushby A. J.; Del Genio A.; Bains W.; Domagal-Goldman S. Exoplanet Biosignatures: A Framework for their Assessment. *Astrobiology* **2018**, 18, 709-738.
12. Fortenberry, R. C.; Huang, X.; Schwenke, D. W.; Lee, T. J. Limited Rotational and Rovibrational Line Lists Computed with Highly Accurate Quartic Force Fields and *Ab Initio* Dipole Surfaces. *Spectrochim. Acta* **2014**, 119A, 76-83.
13. Partridge, H.; Schwenke, D. W. The Determination of An Accurate Isotope Dependent Potential Energy Surface for Water from Extensive Ab Initio Calculations and Experimental Data. *J. Chem. Phys.* **1997**, 106, 4618-4639.
14. Tennyson, J.; Yurchenko, S. N.; Al-Refaie, A. F.; Clark, V. H. J.; Chubb, K. L.; Conway, E. K.; Dewan, A.; Gorman, M. N.; Hill, C.; Lynas-Gray, A. E.; Mellor, T.; McKemmish, L. K.; Owens, A.; Polyanski, O. L.; Semenov, M.; Somogyi, W.; Tinnetti, G.; Upadhyay, A.; Waldmann, I.; Wang, Y.; Wright, S.; Yurchenko, O. P. The 2020 Release of the ExoMol Database: Molecular Line Lists for Exoplanet and Other Hot Atmospheres. *J. Quant. Spectrosc. Radiat. Transfer.* **2020**, 255, 107228.
15. Polyansky, O. L.; Zobov, N. F.; Viti, S.; Tennyson, J.; Bernath, P. F.; Wallace, L. K-band Spectrum of Water in Sunspots. *Astrophys. J. Lett.* **1997**, 489, L205.

16. Huang, X.; Schwenke, D. W.; Lee, T. J. An Accurate Global Potential Energy Surface, Dipole Moment Surface, and Rovibrational Frequencies for NH_3. *J. Chem. Phys.* **2008**, 129, 214304.
17. Huang, X.; Schwenke, D. W.; Lee, T. J. Construction of Spectroscopically Accurate Line lists for NH_3 and CO_2. Proceedings of the 2010 NASA Laboratory Astrophysics Workshop.
18. Huang, X.; Schwenke, D. W.; Lee, T. J. Rovibrational Spectra of Ammonia. Part II: Detailed Analysis, Comparison, and Prediction of Spectroscopic Assignments for $^{14}NH_3$,$^{15}NH_3$, and $^{14}ND_3$. *J. Chem. Phys.* **2011**, 134, 044321.
19. Sung, K.; Brown, L. R.; Huang, X.; Schwenke, D. W.; Lee, T. J.; Coy, S. L.; Lehmann, K. K. Extended line positions, intensities, empirical lower state energies, and quantum assignments of NH_3 from 6300 to 7100 cm^{-1}. *J. Quant. Spectrosc. Radiat. Transfer.* **2012**, 113, 1066-1083.
20. Schwenke, D. W.; Partridge, H. Convergence Testing of the Analytic Representation of an Ab Initio Dipole Moment Function for Water: Improved Fitting Yields Improved Intensities. *J. Chem. Phys.* **2000**, 113, 6592-6597.
21. Huang, X.; Freedman, R, D.; Tashkun, S. A.; Schwenke, D. W.; Lee, T. J. Semi-Empirical $^{12}C^{16}O_2$ IR Line Lists for Simulations Up To 1500K and 20,000 cm^{-1}. *J. Quant. Spectrosc. Radiat. Transfer.* **2013**, 130, 134-146.
22. Huang, X.; Gamache, R. R.; Freedman, R, D.; Schwenke, D. W.; Lee, T. J. Reliable InfraRed Line Lists for 13 CO_2 Isotopologues up to E'=18,000 cm^{-1} and 1500K, with Line Shape Parameters. *J. Quant. Spectrosc. Radiat. Transfer.* **2014**, 147, 134-144.
23. Huang, X.; Freedman, R, D.; Tashkun, S. A.; Schwenke, D. W.; Lee, T. J. Ames-2016 Line Lists for 13 CO_2 Isotopologues: Updates & Remaining Issues. *J. Quant. Spectrosc. Radiat. Transfer.* **2017**, 203, 224-241.
24. Gamache, R. R.; Roller, C.; Lopes, E.; Gordon, I. E.; Rothman, L. S.; Polyansky, O.; Zobov, N. F.; Kyuberis, A. A.; Tennyson, J.; Császár, A. G.; Furtenbacher, T.; Huang, X.; Schwenke, D. W.; Lee, T. J.; Drouin, B.; Tashkun, S. A.; Perealov, V. I. Total Internal Partition Sums for 167 isotopologues of 53 molecules important in planetary atmospheres: application to HITRAN2016 and beyond. *J. Quant. Spectrosc. Radiat. Transfer.* **2017**, 203, 70-87.

25. Huang, X.; Schwenke, D. W.; Lee, T. J. Isotopologue Consistency Consistency of Semi-Empirically Computed Infrared Line Lists and Further Improvement for Rare Isotopologues: CO_2 and SO_2 Case Studies. *J. Quant. Spectrosc. Radiat. Transfer.* **2019**, 230, 222-246.
26. Huang, X.; Freedman, R, D.; Tashkun, S. A.; Schwenke, D. W.; Lee, T. J. Empirical InfraRed Line Lists for Five SO_2 Isotopologues: $^{32/33/34/36}S^{16}O_2$ and $^{32}S^{18}O_2$. *J. Mol. Spectrosc.* **2015**, 311, 19-24.
27. Underwood, D. S.; Tennyson, J.; Yurchenko, S. N.; Huang, X.; Schwenke, D. W.; Lee, T.; Clausen, S.; Fateev, A. J. ExoMol molecular line lists – XIV: The rotation-vibration spectrum of hot SO_2. *Mon. Notices Royal Astron. Soc.* **2016**, 459, 3890-3899.
28. Huang, X.; Schwenke, D. W.; Lee, T. J. Ames $^{32}S^{16}O^{18}O$ Line List for High-Resolution Experimental IR Analysis. *J. Mol. Spectrosc.* **2016**, 330, 101-111.
29. Huang, X.; Schwenke, D. W.; Lee, T. J. Accurate and consistent prediction of molecular IR line lists based on ab initio theory and high-resolution experimental data. *Astronomical Society of the Pacific Conference Series.* **2018**, 515, 155-165.
30. Huang, X.; Schwenke, D. W.; Lee, T. J. Quantitative Validation of Ames IR Intensity and New Line Lists for $^{32/33/34}S^{16}O_2$, $^{32}S^{18}O_2$ and $^{16}O^{32}S^{18}O$. *J. Quant. Spectrosc. Radiat. Transfer.* **2019**, 225, 327-336.
31. Nikitin, A. V.; Rey, M.; Chizhmakova, I. S.; Tyuterev, V. G. First Full-Dimensional Potential Energy and Dipole Moment Surfaces of SF_6. *J. Phys. Chem. A* **2020**, 124, 7014-7023.
32. Raghavachari, K.; Trucks, G. W.; Pople, J. A.; Head-Fordon, M. A Fifth-order Perturbation Comparison of Electron Correlation Theories *Chem. Phys. Lett.* **1989**, *157*, 479-483.
33. Purvis, G. D.; Bartlett, R. J. A full coupled-cluster singles and doubles model: The inclusion of disconnected triples *J. Chem. Phys.* **1982**, *76*, 1910-1918.
34. Lee, T. J.; Scuseria, G. E. Quantum Mechanical Electronic Structure Calculations with Chemical Accuracy; Langhoff, S. R., Ed.; Kleuwer Academic Publishers: Dordrecht, Germany, 1995; pp 47-108.
35. Huang, X.; Lee, T. J. A procedure for computing accurate ab initio quartic force fields: application to HO_2^+ and H_2O, *J. Chem. Phys.,* **2008,** *129*, 044312.

36. Huang, X.; Lee, T. J. Accurate ab initio quartic force fields for NH_2^- and CCH^-, *J. Chem. Phys.*, **2009**, *131*, 104301.
37. Fortenberry, R. C.; Huang, X. ; Francisco, J. S.; Crawford, T. D.; Lee, T. J. The trans-hoco radical: quartic force fields, vibrational frequencies, and spectroscopic constants, *J. Chem. Phys.*, **2011**, *135*, 134301.
38. Martin, J. M. L.; Lee, T. J. The atomization energy and proton affinity of NH_3. An ab initio calibration study, *Chem. Phys. Lett.*, **1996**, *258*, 136.
39. Martin, J. M. L.; Taylor, P. R. Basis Set Convergence for Geometry and Harmonic Frequencies. Are h Functions enough? *Chem. Phys. Lett.* **1994**, *225*, 473-479.
40. Douglas, M.; Kroll, N. M. Quantum Electrodynamical Corrections to the Fine Structure of Helium, *Ann. Phys.* **1974**, *82*, 89-155.
41. Jansen; and Hess, B.A., Revision of the Douglas-Kroll Transformation, *Phys. Rev. A* **1989**, *39*, 6016-6017.
42. Gdanitz, R. J.; Ahlrichs, R. The Averaged Coupled-Pair Functional (ACPF): A Size-Extensive Modification of MRCI(SD). *Chem. Phys. Lett.* **1988**, *143*, 413-420.
43. Dunning, T. H. Gaussian Basis Sets for Use in Corrleated Molecular Calculations. I. The Atoms Boron Through Neon and Hydrogen. *J. Chem. Phys.* **1989**, *90*, 1007-1023.
44. Kendall, R. A.; Dunning, T. H.; Electron Affinities of the First Row Atoms Revisited. Systematic Basis Sets and Wave Functions. *J. Chem. Phys.* **1992**, *96*, 6796-6806.
45. Werner, H.-J., Knowles, P. J.; Manby, F. R.; Sch¨utz, M.; P. Celani, G. Knizia, T. Korona, R. Lindh, A. Mitrushenkov, G. Rauhut, T. B. Adler, R. D. Amos, A. Bernhardsson, A. Berning, D. L. Cooper, M. J. O. Deegan, A. J. Dobbyn, F. Eckert, E. Goll, C. Hampel, A. Hesselmann, G. Hetzer, T. Hrenar, G. Jansen, C. K¨oppl, Y. Liu, A. W. Lloyd, R. A. Mata, A. J. May, S. J. McNicholas, W. Meyer, M. E. Mura, A. Nicklass, P. Palmieri, K. Pfl¨uger, R. Pitzer, M. Reiher, T. Shiozaki, H. Stoll, A. J. Stone, R. Tarroni, T. Thorsteinsson, M. Wang, and A. Wolf, molpro, version 2010.1, a package of ab initio programs, **2015**, see http://www.molpro.net.
46. Dateo, C. E.; Lee, T. J.; Schwenke, D. W. An Accurate Quartic Force Field and Vibrational Frequencies for HNO and DNO. *J. Chem. Phys.* **1994**, *101*, 5853-5859.
47. Fortenberry, R. C.; Huang, X.; Yachmenev, A.; Thiel, W.; Lee, T. J. On the Use of Quartic Force Fields in Variational Calculations. *Chem. Phys. Lett.* **2013**, *574*, 1-12.

48. Rothman, L. S.; Gordon, I. E. E.; Barbe, A.; Benner, D. C. C.; Bernath, P. F. F.; Birk, M.; Boudon, V.; Brown, L. R. R.; Campargue, A.; Champion, J.-P. P.; Chance, K.; Coudert, L. H. H.; Dana, V.; Devi, V. M. M.; Fally, S.; Flaud, J.-M. M.; Gamache, R. R. R.; Goldman, A.; Jacquemart, D.; Kleiner, I.; Lacome, N.; Lafferty, W. J. J.; Mandin, J.-Y. Y.; Massie, S. T. T.; Mikhailenko, S. N. N.; Miller, C. E. E.; Moazzen-Ahmadi, N.; Naumenko, O. V. V.; Nikitin, A. V. V.; Orphal, J.; Perevalov, V. I. I.; Perrin, A.; Predoi-Cross, A.; Rinsland, C. P. P.; Rotger, M.; Šimečková, M.; Smith, M. A. H. A. H.; Sung, K.; Tashkun, S. A. A.; Tennyson, J.; Toth, R. A. A.; Vandaele, A. C. C.; Vander Auwera, J. The HITRAN 2008 Molecular Spectroscopic Database. *J. Quant. Spectrosc. Radiat. Transf.* **2009**, *110* (9–10), 533–572.

49. Schwenke, D. W. Variational Calculations of Rovibrational Energy Levels and Transition Intensities for Tetratomic Molecules. *J. Phys. Chem.* **1996***, 100*(8), 2867-2884; *100*(48), 18884-18884.

50. (a). Schwenke, D. W. New rovibrational kinetic energy operators using polyspherical coordinates for polyatomic molecules. *J. Chem. Phys.* **2003**, *118*(23), 10431-10438. (b). Schwenke D. W. The choice of coordinates for describing vibrations in H_2O. *Chem. Phys. Lett.* **1992**, *189*(1), 91-94.

51. Jaquet, R.; Carrington T. Using a Nondirect Product Basis to Compute J>0 Rovibrational States of H_3^+. *J. Phys. Chem. A* **2013**, 117(39), 9493-9500.

52. Patridge, H.; Schwenke, D. W. The determination of an accurate isotope dependent potential energy surface for water from extensive ab initio calculations and experimental data. *J. Chem. Phys.* **1997**, *106*(11), 4618-4639.

53. Schwenke, D.W. On the computation of high order Rys quadrature weights and nodes. *Comp. Phys. Communi.* **2014**, *185*(3), 762-763.

54. Wolniewicz, L. The $X\,^1\Sigma^+_g$ state vibration - rotational energies of the H_2, HD, and D_2 molecules. *J. Chem. Phys*. **1983**, *78*, 6173-6182.

55. Bunker, P.; Moss, R. The breakdown of the born-oppenheimer approximation: The effective vibration-rotation hamiltonian for a diatomic molecule. *Mol. Phys.* **1977**, *33*(2), 417-424.

56. Schwenke, D. W. Beyond the Potential Energy Surface: Ab initio Corrections to the Born-Oppenheimer Approximation for H_2O. *J. Phys. Chem. A* **2001**, *105*(11), 2352-2360.

57. (a) Schwenke, D. W.; Patridge, H. Vibrational energy levels for CH_4 from an ab initio potential. *Spectrochimica Acta Part A* **2001**, *57*(4), 887-895. (b) Schwenke, D. W. Towards accurate ab initio predictions of the vibrational spectrum of methane", *Spectrochimica Acta A*, **2002**, *58*, 849.
58. Schwenke, D. W. *private communication.*
59. Schwenke, D. W. A unified derivation of Hamiltonian and optical transition matrix elements for open shell diatomic and polyatomic molecules using transformation tools of modern quantum mechanics. *J. Chem. Phys.* **2015**, *142*(14), 144107.
60. Yurchenko, S. N.; Barber, R. J.; Yachmenev, A.; Thiel, W.; Jensen, P.; Tennyson, J. A Variationally Computed T = 300 K Line List for NH_3. *J. Phys. Chem. A* **2009**, *113* (43), 11845–11855.
61. Hu, C; Perevalov, V. I.; Cheng, C.; Hua, T.; Liu, A.; Sun, Y.; Tan, Y.; Wang, J.; Hu, S. Optical–Optical Double-Resonance Absorption Spectroscopy of Molecules with Kilohertz Accuracy. *J. Phys. Chem. Lett.* **2020**, *11*(18), 7843-7848.
62. Tashkun, S. A.; Perevalov, V. I.; Gamache, R. R.; Lamouroux, J. CDSD-296, high-resolution carbon dioxide spectroscopic databank: An update. *J. Quant. Spectrosc. Radiat. Transfer.* **2019**, *228,* 124-131.
63. Čermák, P.; Karlovets, E.; Mondelain, D.; Kassi, S.; Perevalov, V. I.; Campargue, A. High sensitivity CRDS of CO_2 in the 1.74 μm transparency window. A validation test for the spectroscopic databases. *J. Quant. Spectrosc. Radiat. Transf.* **2018***, 207,* 95–103.
64. Evseev, V.; Fateev, A.; Clausen, S. High-resolution transmission measurements of CO_2 at high temperatures for industrial applications*. J Quant. Spectrosc. Radiat. Transfer* **2012**, *113,* 2222–2233.
65. Ulenikov, O. N.; Bekhtereva, E.; Krivchikova, Y.; Zamotaeva, V.; Buttersack, T.; Sydow, C.; Bauerecker, S. Study of the high resolution spectrum of $^{32}S^{16}O^{18}O$: The ν_1 and ν_3 bands. *J Quant. Spectrosc. Radiat. Transfer* **2016**, *168,* 29–39.